Electronically supporting information

Fabrication of dual-fluorescent hybrid material based on post-modification of covalent organic frameworks for the detection of herbicides and the design of a smartphone sensing platform

*Xiaoqin Shen, Bing Yan**

School of Chemical Science and Engineering, Tongji University, Siping Road 1239, Shanghai 200092, China.

1. Experimental Section

---

* Corresponding author: Email address: byan@tongji.edu.cn (Bing Yan)

1.1. Materials

$Tb(NO_3)_3 \cdot 6H_2O$ was prepared by dissolving Tb_2O_3 into excess nitric acid with continuous magnetic stirring, followed by evaporation and crystallization several times. All the other solvents and reagents were obtained commercially and used without further purification. Deionized water was used throughout the experiments. 2,4,6-Triformylphloroglucinol (Tp) (98%), 4,4′,4′′-(1,3,5-triazine-2,4,6-triyl)trianiline (Tta) (98%), 2,2′:6′,2′′-terpyridine (Terpy) (98%), Glyphosate (Gly) (96%), glufosinate (Glu) (97%), aminomethylphosphonic acid (AMPA) (99%), falisilvan (98%), rimsulfuron (96%), nicosulfuron (95%), alidochlor (97%), polyvinylidene fluoride (PVDF) were purchased from Adamas-beta. $NaHCO_3$ (99%), NaCl (99%), KCl (99%), $MgCl_2$ (99%), $CaCl_2$ (96%), Na_2SO_4 (99%) were purchased from Sigma-Aldrich. Falisilvan (98%), flumioxazin (99%), flusilazole (98%), tepraloxydim (99%), 2,3-dichlorophenoxyacetic (98%) were purchased from Aladdin Chemistry. $NaNO_3$ (99%), 1,4-dioxane (99.5%), *N*, *N*-dimethylformamide (99.5%) and dichloromethane (99.8%) were purchased from Greagent.

1.2. Instruments

The powder X-ray diffraction (PXRD) patterns were recorded on Bruker D8 ADVANCE diffractometer employing Cu Kα radiation (40 mA and 40 kV) with a 2θ range from 3° to 45° at room temperature. The surface morphology and EDS analysis were performed on Hitachi S-4800 field emission scanning electron microscope (SEM) with a voltage of 5 kV-15 kV. Fourier transform infrared (FT-IR) spectra were obtained by a Nexus 912 AO446 infrared spectrum radiometer in the wavenumber range of 4000 - 400 cm^{-1}. X-ray photoelectron spectroscopy (XPS) spectra were noted under the ultrahigh vacuum ($< 10^{-6}$ Pa) at pass energy (93.90 eV) with Axis Ultra DLD spectrometer (Kratos, Japan) by employing an Mg Kα (1253.6 eV) anode. Thermogravimetric (TG) curves were measured on a TA TGA 55 system operating at a heating rate of 10 ^{o}C/min in the range of 25 ^{o}C up to 800 ^{o}C under N_2 atmosphere. The fluorescence spectra were obtained on an Edinburgh FLS920 spectrophotometer employing 450 W xenon lamp as the source of excitation with appropriate cutoff filter. The Commission International de I'Eclairage (CIE) coordinate were calculated by CIE1931 chromaticity coordinate calculation according to the fluorescence emission spectra. The UV-vis absorption spectra were carried on an Agilent 8453 spectrometer. The pH values of aqueous solutions were determined by an INESA PHS-25 pH meter with an E-201F pH composite electrode, which was carefully calibrated by standard buffer solution before testing. The HOMO-LUMO orbital energies were optimized by the B3LYP hybrid density functional and the basis set was 6-31G (d).

1.3. Synthesis of TpTta

TpTta were synthesized according to the previous report.[S1] Briefly, Tp (0.15 mmol), Tta (0.15 mmol), 3 mL of dioxane and 0.25 mL of 6 M aqueous acetic acid was mixed in a 10 mL Schlenk tube. After sonicated for 10 min, the tube was degassed by three freeze-pump-thaw cycles and sealed off. Upon warming to room temperature, the tube was placed in an oven at 120 ºC and left undisturbed for 3 days The precipitate was collected by centrifugation and washed with DMF thrice and DCM twice. The collected powder was dried in vacuum overnight.

2. Supporting Figures and Tables

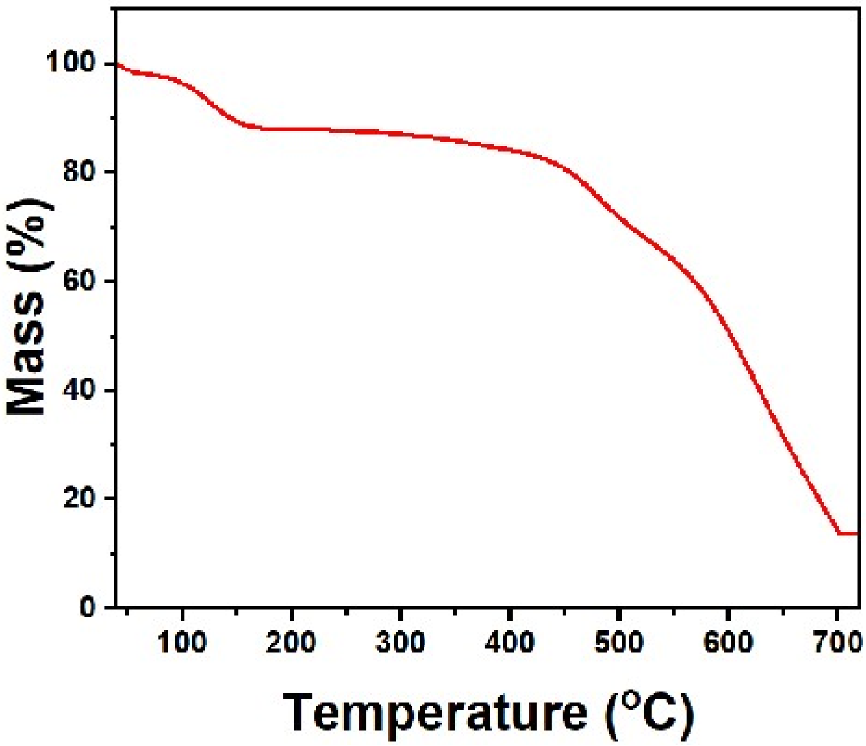

Fig. S1 TGA analysis of TpTta.

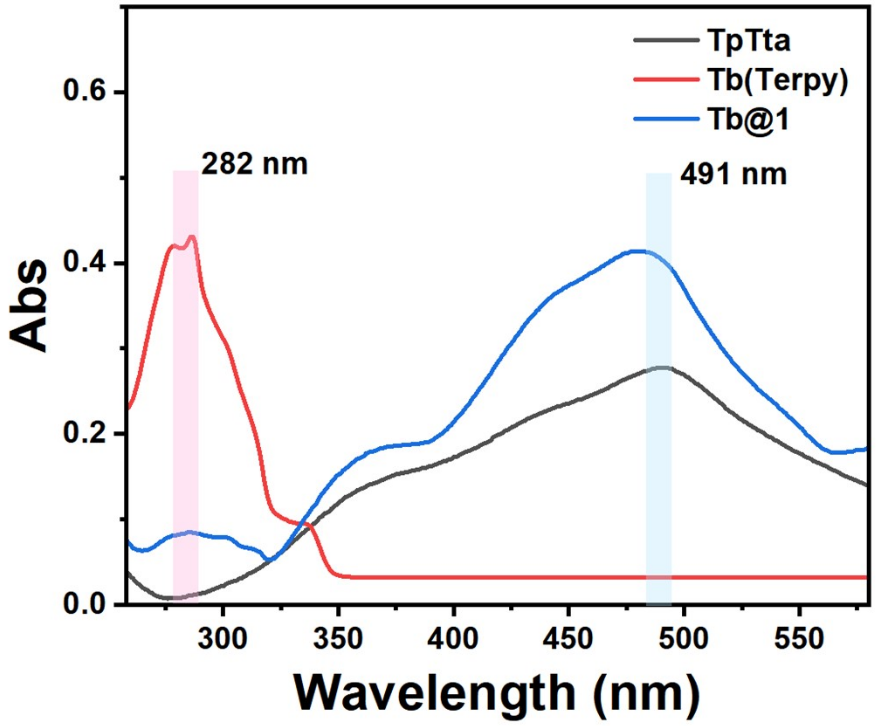

Fig. S2 The UV-vis spectra of TpTta, Tb(Terpy) and Tb@1.

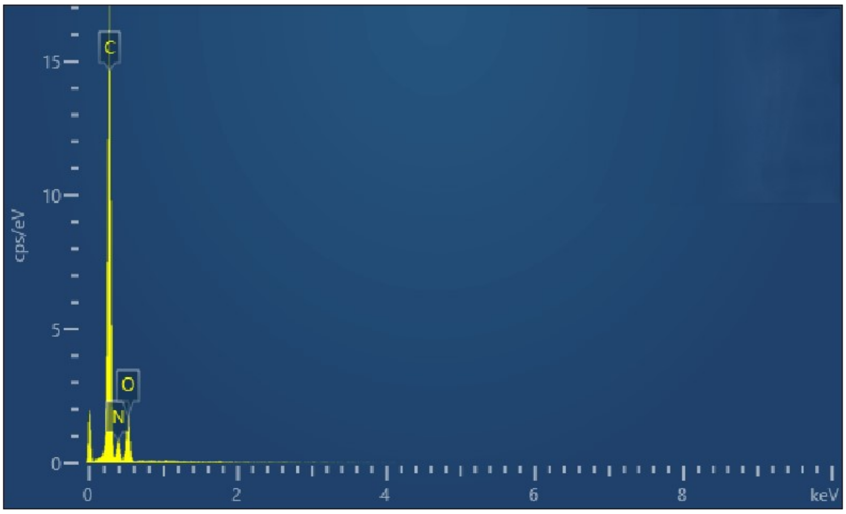

Element	Wt %	Wt% Sigma
C	74.0	0.8
N	12.9	0.9
O	13.2	0.5

Fig. S3 EDS analysis of TpTta.

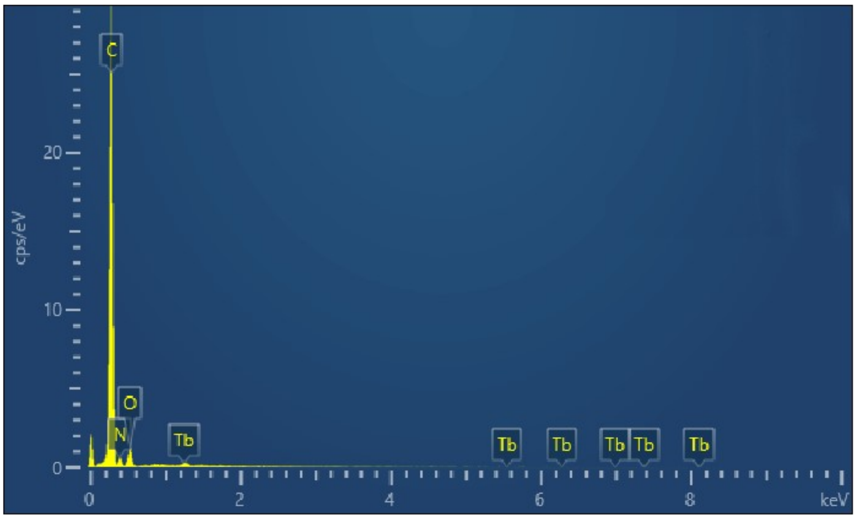

Element	Wt %	Wt% Sigma
C	76.9	0.7
N	12.5	0.7
O	8.4	0.3
Tb	2.3	0.3

Fig. S4 EDS analysis of Tb@1.

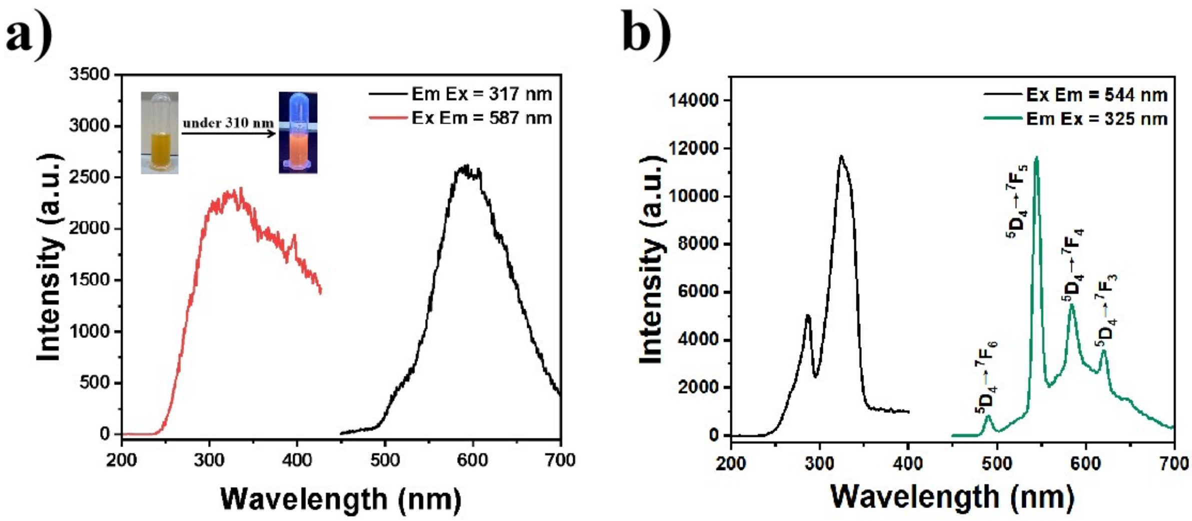

Fig. S5 a) Excitation and emission spectra of TpTta; b) Excitation and emission spectra of Tb@1.

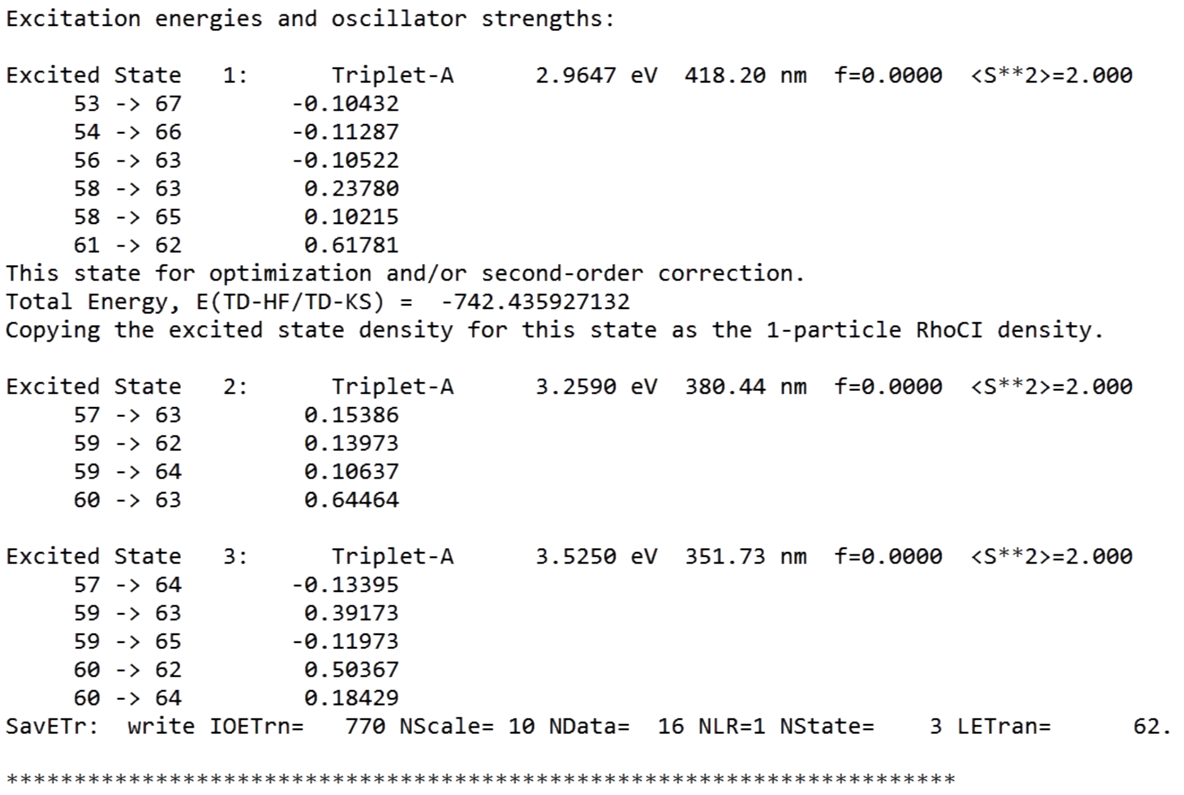

```
Excitation energies and oscillator strengths:

Excited State   1:      Triplet-A      2.9647 eV  418.20 nm  f=0.0000  <S**2>=2.000
     53 -> 67        -0.10432
     54 -> 66        -0.11287
     56 -> 63        -0.10522
     58 -> 63         0.23780
     58 -> 65         0.10215
     61 -> 62         0.61781
This state for optimization and/or second-order correction.
Total Energy, E(TD-HF/TD-KS) =  -742.435927132
Copying the excited state density for this state as the 1-particle RhoCI density.

Excited State   2:      Triplet-A      3.2590 eV  380.44 nm  f=0.0000  <S**2>=2.000
     57 -> 63         0.15386
     59 -> 62         0.13973
     59 -> 64         0.10637
     60 -> 63         0.64464

Excited State   3:      Triplet-A      3.5250 eV  351.73 nm  f=0.0000  <S**2>=2.000
     57 -> 64        -0.13395
     59 -> 63         0.39173
     59 -> 65        -0.11973
     60 -> 62         0.50367
     60 -> 64         0.18429
SavETr:  write IOETrn=   770 NScale= 10 NData=  16 NLR=1 NState=    3 LETran=      62.

**********************************************************************
```

Fig. S6 The result of Gaussian calculation of Terpy.

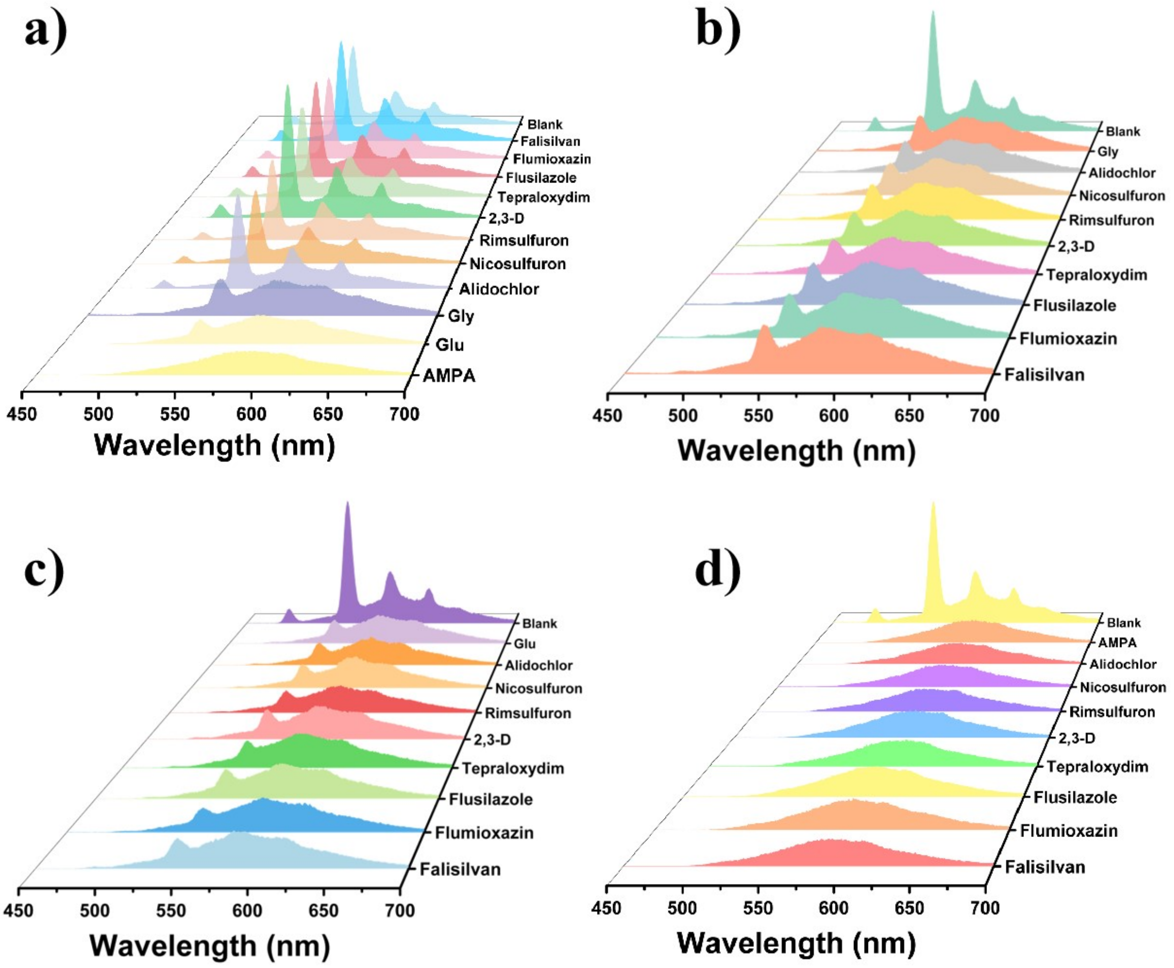

Fig. S7 Emission spectra of the luminescence response of Tb@1 toward Gly, Glu and AMPA in the absence and presence of other herbicides.

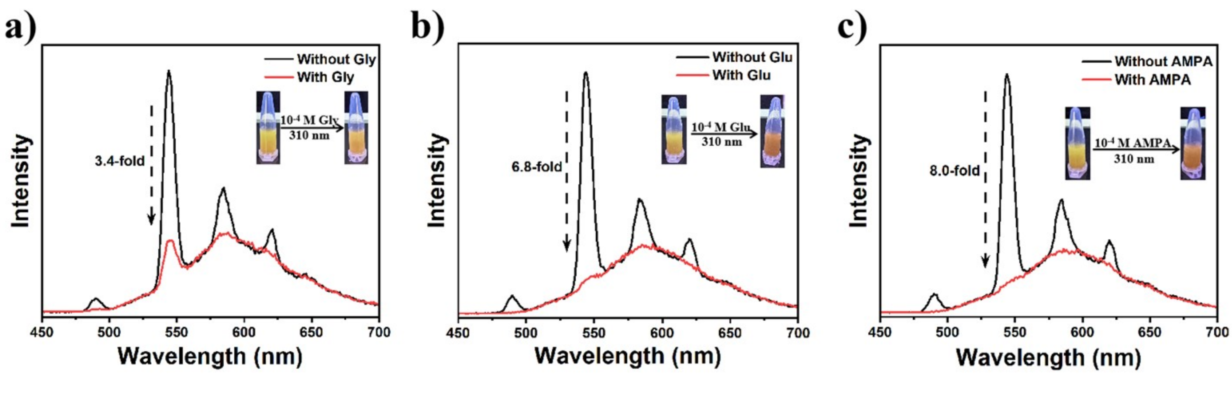

Fig. S8 Fluorescence spectra of Tb@1 a) with and without 10^{-4} M Gly; b) with and without 10^{-4} M Glu; c) with and without 10^{-4} M AMPA (λ_{ex} = 325 nm).

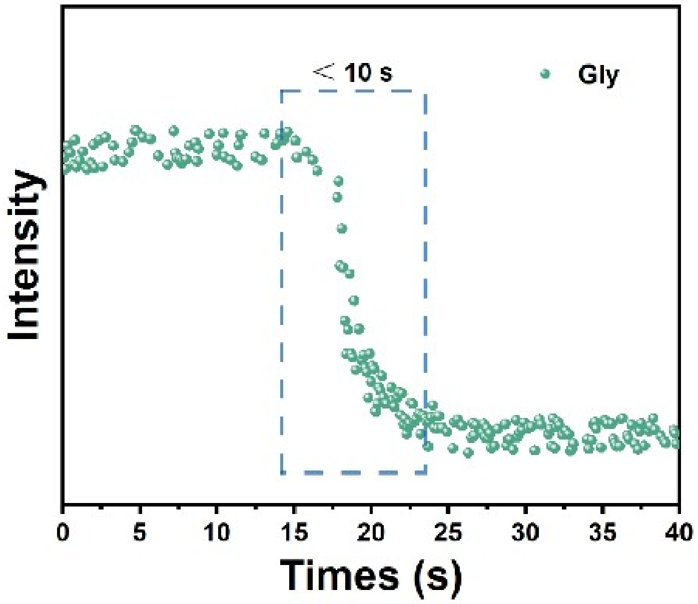

Fig. S9 Response time of Tb@1 to Gly.

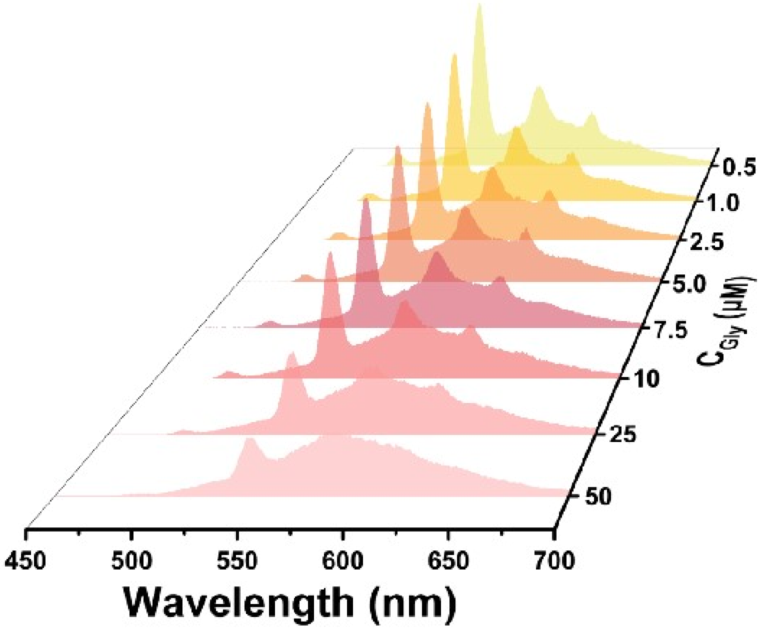

Fig. S10 The emission spectra of Tb@1 upon the gradual addition of Gly.

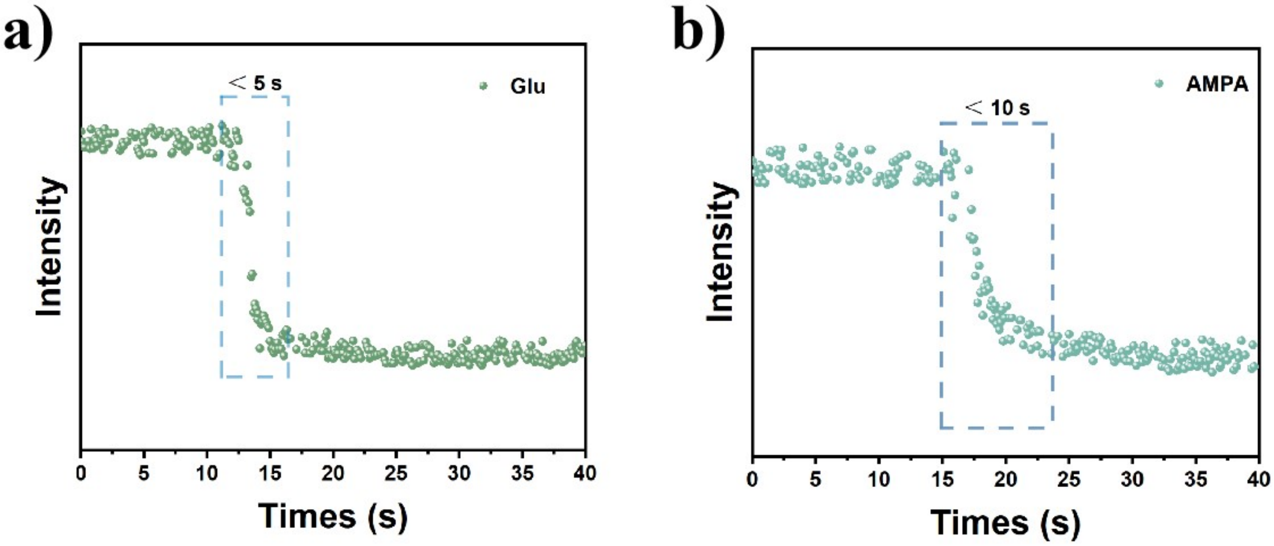

Fig. S11 Response time of Tb@1 to a) Glu; b) AMPA.

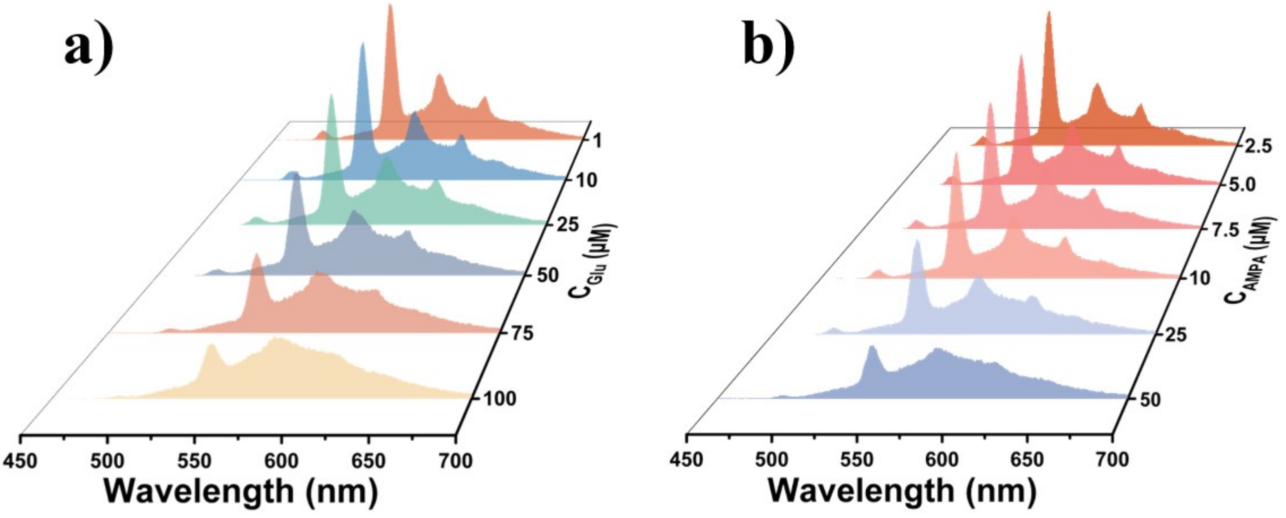

Fig. S12 The emission spectra of Tb@1 upon the gradual addition of a) Glu; b) AMPA.

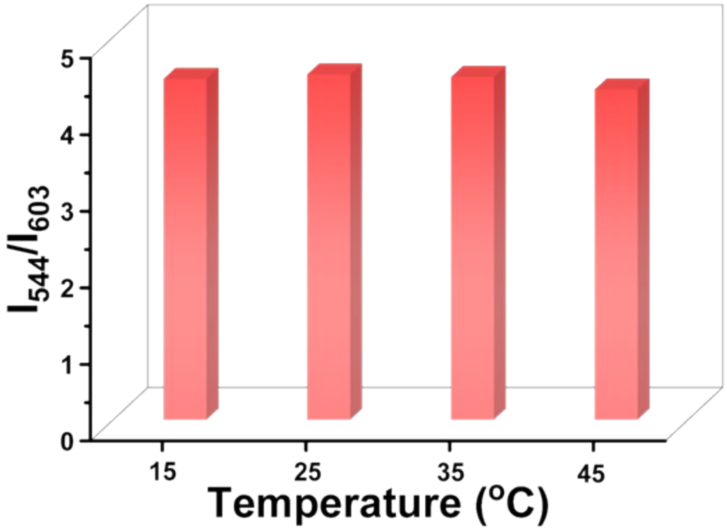

Fig. S13 Variation of fluorescence intensity ratio of Tb@1 at different temperatures.

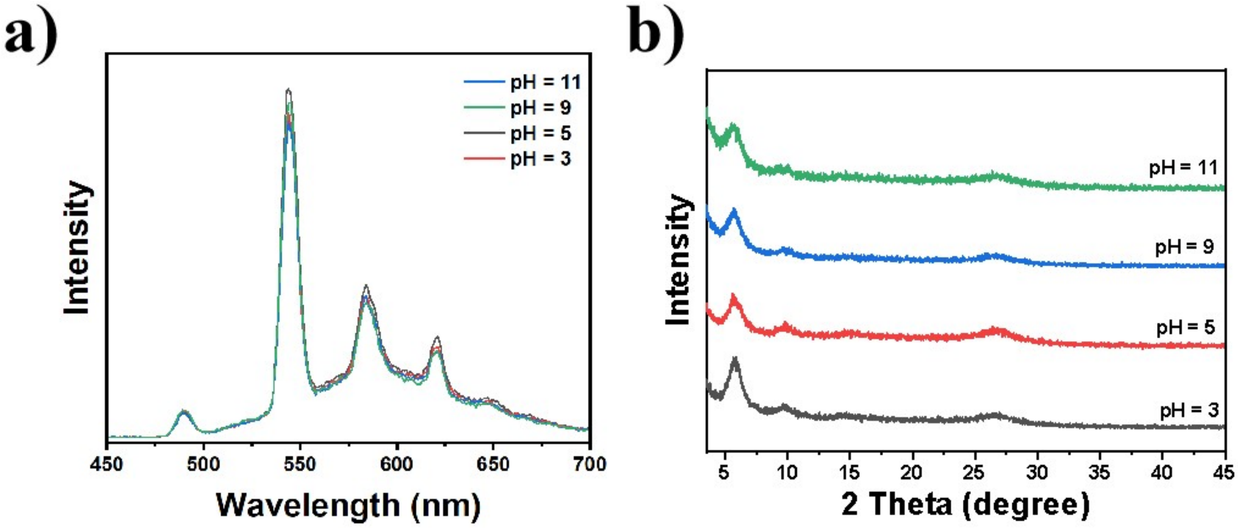

Fig. S14 a) Variation of fluorescence intensity of Tb@1 and b) PXRD patterns of Tb@1 after soaking in different pH solutions for 24 h.

Fig. S15 Sketching map of synthetic process of thin film.

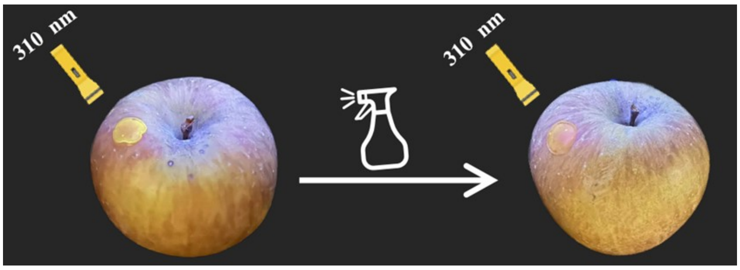

Fig. S16 Rapid and visible imaging of AMPA applied on the surface of apple produce.

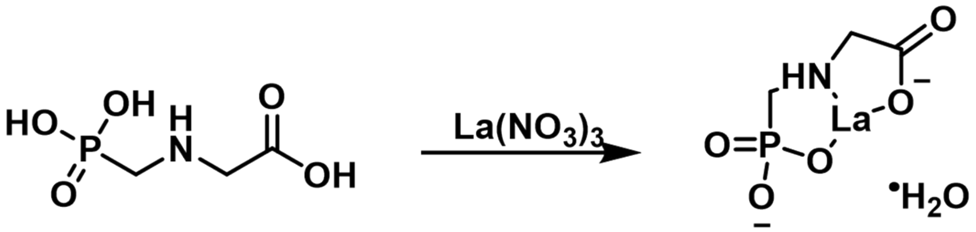

Scheme S1 Reaction of Gly and $La(NO_3)_3$.

Table S1 Summary of the methods for sensing Gly, Glu and AMPA

Analyte	Method	Linear range/µM	LOD/µM	Ref
Gly	Capillary Electrophoresis	1.5–300	0.8	[S2]
Gly	Fluorescence	11.83–118.3	0.61	[S3]
Gly	Fluorescence (CDs)	2.0–20	0.6	[S4]
Gly	capillary electrophoresis	13–1600	1.2	[S5]
Gly	ICP-MS	0.5–20	0.6	[S6]
Gly	MSPE-HPLC	0.43–11.83	0.124	[S7]
Gly	Surface Plasmon Resonance Sensor	0–0.59	0.008	[S8]
Gly	Fluorescence	0.5–50	0.033	This work
Glu	Capillary Electrophoresis	1.5–300	0.8	[S2]
Glu	capillary electrophoresis	6–1970	0.6	[S5]
Glu	ICP-MS	2.4–20	3.9	[S6]
Glu	MSPE-HPLC	0.35–9.29	0.105	[S7]
Glu	Fluorescence	4.65–116.18	0.05	[S9]
Glu	Fluorescence	1–100	0.11	This work
AMPA	Capillary Electrophoresis	1.5–300	0.9	[S2]
AMPA	capillary electrophoresis	38–1890	1.7	[S5]
AMPA	ICP-MS	2.2–20	6.3	[S6]
AMPA	MSPE-HPLC	0.66–18.01	0.198	[S7]
AMPA	Fluorescence	2.5–50	0.26	This work

References

[S1] W. Li, C. Yang and X. Yan, *Chemical Communications*, 2017, **53**, 11469-11471.

[S2] S. Chang and M. Wei, *J. Chin. Chem. Soc.*, 2005, **52**, 785-792.

[S3] Q. Li, Y. Guo, X. He and G. Li, *Talanta,* 2023, **265**, 124865.

[S4] Y. Yuan, J. Jiang, S. Liu, J. Yang, H. zhang, J. Yan and X. Hu, *Sens. Actuators B Chem.*, 2017, **242**, 545-553.

[S5] S. Chang and C. Liao, *J. Chromatogr. A*, 2002, **959**, 309-315.

[S6] Y. Kazui, Y. Seto and H. Inoue, *Forensic Toxicol.*, 2014, **32,** 317-322.

[S7] N. Surapong and R. Burakham, *ACS Omega*, 2021, **6**, 27007-27016.

[S8] M. H. Do, B. Dubreuil, J. Peydecastaing, G. Vaca-Medina, T. T. Nhu-Trang, N. Jaffrezic-Renault and P. Behra, *Sensors* 2020, **20**, 5942

[S9] F. Y. Zhu, J. Zhu and Z. Z. Zhang, *RSC Adv.*, 2017, **7**, 48077-48082.